Modelling, Simulation and Control of Smart and Connected Communities

Zhaoxuan Li[1], Ankur Pipri[2], Bing Dong[1], Nikolaos Gatsis[2], Ahmad F. Taha[2], Nanpeng Yu[3]
[1]Department of Mechanical Engineering, University of Texas at San Antonio, San Antonio, Texas, U.S.A
[2]Department of Electrical and Computer Engineering, University of Texas at San Antonio, San Antonio, Texas, U.S.A
[3]Department of Electrical and Computer Engineering, University of California Riverside, Riverside, California, U.S.A

Abstract

This study attempts to establish the need for a framework to assess the impact of connected buildings in a smart community. The contribution is a software framework designed to optimize buildings and grids at a district level. The following research products are developed: (1) An innovative method to model a cluster of buildings—with people's behavior embedded in the cluster's dynamics—and their controls so that they can be integrated with grid operation and services; (2) a novel optimization framework to solve complex, centralized control problems for large-scale systems, leveraging convex programming approaches; and (3) a methodology to assess the impacts of connected buildings in terms of (a) the grid's operational stability and safety and (b) buildings' optimized energy consumption. To test the proposed framework, a large-scale simulation of a subtransmission network with three power generating stations and serving over 300 artificial buildings is conducted.

Introduction

It is well realized that two-thirds of global primary energy consumption can be attributed to cities, leading to 75% of world energy production and generating 80% of greenhouse gas emissions (Lazaroiu, 2012). Nowadays, nations across world are proposing a new urban district model, "the smart city," to increase the connection, sustainability, comfort, attractiveness and security among the urban communities. It will play an important role in reducing global energy consumption, curbing greenhouse gas emissions, and maintaining stable electric-grid operations. Humans spend more than 90% of their time in buildings and profoundly influence the smart controls of the buildings. Recent research studies have addressed a breadth of optimization, control and occupancy-related challenges to the design and operation of buildings and power networks. In particular, a line of prior studies model urban scale building energy performance, where physical models of heat and mass flows in and around buildings are developed and applied to predict operational energy as well as indoor and outdoor environmental conditions for groups of buildings (Howard, 2012; Heiple, 2008; Reinhart, 2016). The bulk of the recent literature on this topic focused on studying the reduction in building energy consumption with occupancy and behaviour prediction. Other studies addressed the integration of smart building into the smart distribution grid (Zhao, 2015; Blum, 2014; Pisello, 2012).

However, few of the existing work has studied the interplay among buildings, power grids, and people in a holistic framework (Chatzivasileiadis, 2016). Consequently, ARPA-E, the International Energy Agency, and U.S. DOE all stress the need to build modern grids and infrastructures that all operate as one (ARPA-E,2016). As buildings are physically connected to the electric power grid, it is a natural idea to understand the coupling of decisions and operations between the two. However, at a community level, there is no holistic framework that buildings and power grids can simultaneously utilize to optimize their performance. The challenges related to establishing such a framework at a community level are: a) lack of a holistic, multi-time scale mathematical framework that couples the real-time decisions of buildings and grid stakeholders; and b) lack of a computationally-tractable solution methodology amenable to implementation on a large number of connected power grid-nodes and buildings (commercial and residential buildings).

In this paper, the author plans to investigate a novel mathematical framework that fills the aforementioned knowledge gaps, and tests the following hypothesis: Connected buildings, people, and grids will achieve significant energy savings and stable operation within a smart and connected community. This framework will integrate individual building dynamics and power grid coupling by using a centralized Model Predictive Control approach.

Building Dynamics

Individual building energy consumption models such as EnergyPlus (Energyplus, 2015) and eQuest (Equest, 2016) have been developing for decades where the fundamentals of heat transfer and thermal dynamics are accurately captured. The complexity and high number of model variables make these models difficult to include in large-scale smart community modeling and optimization. Recently, researchers developed reduced order thermal network models to solve the individual building optimal control problem (Dong, 2014). However, this reduced order model is still too complex when hundreds of heterogeneous buildings need to be modeled

https://doi.org/10.26868/25222708.2017.634

simultaneously. In this project, the authors will develop a further reduced order thermal resistance and capacitance (RC) network model which only has two temperature states, namely, space temperature T_{zone} and structure temperature T_{wall}, for each building, as depicted in Figure 1.

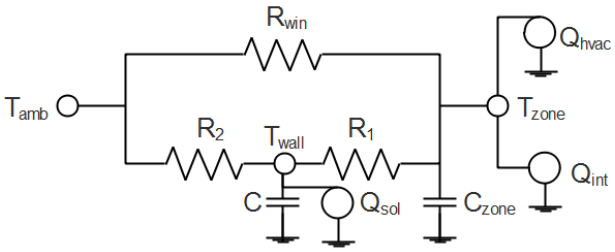

Figure 1: 2R1C Thermal Network.

From Figure 1, the temperature states, T_{wall}, and T_{zone}, of the "super-zone" are given by:

$$C\dot{T}_{wall}(t) = \frac{T_{amb}(t) - T_{wall}(t)}{R_2} + \frac{T_{zone}(t) - T_{wall}(t)}{R_1} + Q_{sol}(t)$$

$$C_{zone}\dot{T}_{zone}(t) = \frac{T_{wall}(t) - T_{zone}(t)}{R_1} + \frac{T_{amb}(t) - T_z}{R_{win}} + Q_{int}(t) + Q_{hvac}(t) \quad (1)$$

Where:

- R_{win}, R_2, and R_1 are the physical parameters of the building envelope;
- C is a lumped thermal capacity of all walls and roof;
- C_{zone} is the thermal capacity of the zone;
- $Q_{sol}(t)$ is the total absorbed solar radiation on the external wall;
- $Q_{int}(t)$ is the total internal heat gains from space heat sources such as desktop, people, lights, etc;
- $T_{amb}(t)$, $T_{zone}(t)$, and $T_{wall}(t)$ are the outside ambient, zone, and wall temperatures, respectively;
- $Q_{hvac}(t)$ is the ideal cooling source;

Hence, the dynamics of building l in state-space format can be written as:

$$\dot{x}^l = A_x^l x^l + B_{u_x}^l u_x^l + B_{w_x}^l w_x^l \quad (2)$$

Where the state, input, and disturbance vectors are given as follows:

$$x^l = [T_{wall}\ T_{zone}]_l^T,$$
$$u_x^l = [P_{hvac}]_l,$$
$$w_x^l = [T_{amb}\ Q_{sol}\ Q_{int}]_l^T$$

And the system matrices are defined in as follows:

$$A_x^l = \begin{bmatrix} -\frac{1}{C}\left(\frac{1}{R_1}+\frac{1}{R_2}\right) & \frac{1}{CR_1} \\ \frac{1}{C_{zone}R_1} & -\frac{1}{C_{zone}}\left(\frac{1}{R_1}+\frac{1}{R_{win}}\right) \end{bmatrix},$$

$$B_{u_x}^l = \begin{bmatrix} 0 \\ \frac{1}{C_{zone}} \end{bmatrix}, B_{w_x}^l = \begin{bmatrix} \frac{1}{CR_2} & \frac{1}{C} & 0 \\ \frac{1}{C_{zone}R_{win}} & 0 & \frac{1}{C_{zone}} \end{bmatrix}$$

The system description (2) represents a linear, time-invariant dynamical system for the building l, where:

- x^l is the state-vector;
- u_x^l is the controllable input control-vector;
- w_x^l is the known, yet uncontrollable input

For the integration between buildings and grids, the global dynamics of a cluster of the buildings need to be expanded from a single building, such as the building l from Equation (2). It is assumed that all buildings are operating with same time-scales of the power system dynamics. If there are no connections between buildings, the global state-space dynamics of the building cluster comprised of a total of n buildings can be derived as follows:

$$\dot{X}_b(t) = A_X X_b(t) + B_{u_X} U_X(t) + B_{w_X} W_X(t) \quad (3)$$

Where:

- X_b=$[x^1, x^2, \dots, x^n]$, U_X=$[u_X^1, u_X^2, \dots, u_X^n]$; W_X=$[w_X^1, w_X^2, \dots, w_X^n]$;
- A_X=diag$(A_x^1, A_x^2, \dots, A_x^n)$;
- B_{UX}=diag$(B_{u_x}^1, B_{u_x}^2, \dots, B_{u_x}^n)$;
- B_{WX}=diag$(B_{w_x}^1, B_{w_x}^2, \dots, B_{w_x}^n)$.

Power System Dynamics

In this section, the swing equation defines the dynamic transfer of energy between generators and loads. The swing equation models the dynamical behavior of the k_{th} bus with M_k and D_k as the inertia and damping coefficients in a power network, which relates the phase angle, δ (the rotor angle with respect to a rotating reference frame which rotates at synchronous speed ω_s) with the angular velocity $\dot{\delta}$, and angular acceleration, $\ddot{\delta}$. The synchronous speed ω_s corresponds to the grid frequency of 60 Hz in North America via the relationship ω_s=$2\pi 60$ rad/sec. Let $P_{k,j}$ be the active power flow from the k^{th} to the j^{th} node; and Let n to be the number of nodes in the network. The swing equation is expressed as follows:

$$M_k\ddot{\delta}_k(t) + D_k\dot{\delta}_k(t) = P_m^k(t) - P_k(t) - \sum_{j=1,\dots,n} P_{k,j}(t) \quad (4)$$

Where:

- P_m^k is the mechanical input power at bus k;
- P_k is the total load at bus k;
- $P_{k,j}$ is the linearized power flow from the generator j.

If there is no generator on bus k, then we set M_k and D_k to zero, while the control variable P_m^k can either be eliminated, or constrained to be zero. Let b_{kl} be 1 if building l is connected to bus k, and 0 otherwise; Let L to be the total building number Then, P_k and $P_{k,j}$ can be expressed as:

$$\begin{cases} P_{k,j} = a_{kj}(\delta_k(t) - \delta_j(t)) \\ P_k = F_{D_k}\dot{\delta}(t) + F_k + \sum_{l=1}^{L} b_{kl}(P_{hvac}^l + P_{mi}^l) \end{cases} \quad (5)$$

Where:

- a_{kj} is a parameter of the transmission line connecting buses k and j that converts angle differences to power flows (Taylor, 2015; Gatsis, 2013); a_{kj}=0 if there is no line connecting buses k and j;
- $F_D\dot{\delta}(t)$ is the frequency-sensitive uncontrollable load at bus k;

- F_k is the frequency-insensitive uncontrollable load at bus k;
- P^l_{hvac} is calculated from Equation 2 and P^l_{mi} is the miscellaneous load of building l with no potential contribution in frequency regulation.

Let $\dot{\delta}_k = \omega_k$. Then the second order Equation (4) for the bus k can be equivalently written as two first order differential equations. The augmented power dynamics for all buses then can be written as the following state-space equations:

$$E\dot{X}_g(t) = A_g X_g + A_{hvac}U_{hvac}(t) + B_m U_m(t) + B_F U_F(t) + B_{mi}W_{mi}(t) \quad (6)$$

Where:

- $X_g(t) = [\delta^1, \delta^2, \dots, \delta^n, \omega^1, \omega^2, \dots, \omega^n]$;
- $U_{hvac} = [P^1_{hvac}, P^2_{hvac}, \dots, P^L_{hvac}]$;
- $U_m = [P^1_m, P^2_m, \dots, P^n_m]$
- $U_F = [F_1, F_2, \dots, F_n]$;
- $W_{mi} = [P^1_{mi}, P^2_{mi}, \dots, P^L_{mi}]$;

Integrated Framework of Controls

An objective of the framework to be developed is to generate local control actions/signals for buildings and power generators such that the overall performance is optimized—in terms of stability, energy savings, and other socioeconomic metrics. However, the formulated dynamics in Equation (3) and Equation (6) clearly operate on two different time-scales. While the grid controls and states are often in milliseconds and seconds, the building state dynamics and controls are much slower, often in minutes. Especially the AC loads and temperatures in buildings change slowly in comparison with angles, frequencies, and voltages. However, the problem is still coupled because when electric motor loads in buildings' response to grid frequency regulation, it will have long-term impacts on building thermal loads. For example, a frequency regulated fan will have impacts on total amount of cooling loads into spaces.

To overcome this limitation, the authors make the local optimal control laws for buildings to compute at different time-steps than local optimal control laws for generators. This approach mimics the physical realities for these systems, and this consideration can be imposed via constraints in the optimal control problem. Hence, the objective of this task is to construct these constraints. Since buildings possess slower dynamic behavior, the authors restrict the controls and states of buildings to depict the time-scales discrepancy. These constraints are then added to the joint optimal control formulation proposed.

The proposed optimal control formulation is based on the well-known linear quadratic regulator (LQR) problem for nonlinear dynamical systems. The LQR formulation for classical power systems has been adapted before (Taylor, 2015; Fosha, 1970; Elgerd, 1970). Furthermore, an LQR-like cost function has been applied to commercial building (Maasoumy, 2014; Ma, 2009)—hence our choice of the LQR as an optimal control routine. The general form of the global optimal control problem can be written as follows:

$$\begin{aligned} &\text{minimize } \int_{t_o}^{t_f} C(x,u,w)\, dt \\ &\text{subject to } \dot{x} = A_x x(t) + B_u u(t) + B_w w(t) \\ &u^{min} \le u(t) \le u^{max} \\ &x^{min} \le x(t) \le x^{max} \\ &u_b(t) \in U_b,\ x_b(t) \in X_b. \end{aligned} \quad (7)$$

Where:

- $x(t)$ includes $X_b(t)$ and $X_g(t)$
- $u(t)$ includes $U_{hvac}(t)$ and $U_m(t)$
- The cost functional C penalizes the cost of the operation of the buildings and the grid dynamics. This cost models economic and social-technical objectives such as: discomfort in reducing the temperature in individual buildings, the deviations in the frequency of the power system, the cost of applying a building or generator control, the high disturbances, and the potential cost on communication between different components.
- The first three constraints in Equation (7) depict the integrated dynamics, and bounds on the states and control actions.
- The last constraint in Equation (7) corresponds to the time-scales discrepancies between grid and building controls and states. Specifically, $u_b(t) \in U_b$ signifies that during the faster time-scale corresponding to the grid, the building controls are held constant — these feasible regions U_b and X_b are constructed globally when integrating building and power grid.

The optimization problem (7) cannot be solved analytically as it is a nonlinear optimal control problem with generally nonconvex constraints. The objective of the following section is to investigate and develop optimal control solutions for different solution methodologies. In addition, and to address the time-scale discrepancy, a two-level Model Predictive Control (MPC) scheme will be developed, whereby the control laws for the slower and faster processes will be jointly computed; the time-steps of the latter will be nested in the time-steps of the former, while the joint system states evolve according to the coupling modeled by Equation (3) and (6). This approach will be tested by combining with appropriate linearization of building and grid nonlinearities.

Previous work on the design and analysis of perturbed decentralized networked control systems (Elmahdi, 2015; Taha, 2015) have demonstrated the possibility achieve the goals of controls by using a decentralized approach. Distributed approach is also possible by utilizing their prior expertise in dual decomposition and subgradient methods (Gatsis, 2012; Gatsis 2014), disaggregated cutting plane and bundle methods (Gatsis, 2013; Zhang, 2013)), or the alternating-direction method of multipliers (ADMM) (Bazrafshan, 2016). However, only a centralized approach is proposed for demonstration purpose in this study for different system-level scenarios, illustrated in Figure 2. The resulting optimization problem will be a large-scale linear or quadratic program

(depending on the building and grid cost functions), which will be tractable for a smaller community-scale system. This approach will naturally not be feasible for systems with larger number of buildings, while privacy concerns of building operators will likely not allow collecting all relevant building parameters and control constraints to the system operator.

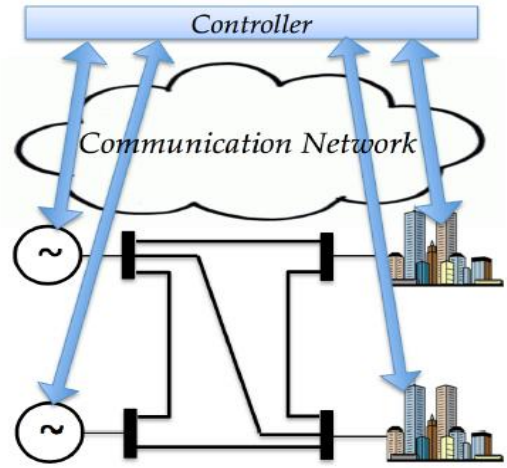

Figure 2: The control and optimization architectures.

In summary, there are three challenges for the integrated framework to be functional in optimizations for large scale simulation at the community level. First, controls of the states of buildings and grids have significant time-scales discrepancy. An innovative discretization of systems between the two time scales (buildings and grids) needs to be utilized when discretize building parameters to building-grid optimization. Second, fast and feasible optimization programmings need to be proposed so that hundreds of buildings can be integrated to multiple grid buses. Third, the occupancy comfort and grid frequency constrained should not be violated. How to build a proper large-scale optimization algorithm and the suitable cost function need to be modeled and evaluated clearly. Every coupling among the occupancy, the buildings and the grid require explicit mathematical expressions in the entire integrated framework.

Centralized Approach

In this section, the authors investigate the discrepancies in time-scales between the building and power network dynamics, and discuss an MPC-based formulation of the joint optimal control problem that (a) addresses the time discrepancies of buildings and (b) incorporates frequency regulation routine based on the coupling of building loads with the power system dynamics.

First, the authors discuss the optimal control problem of buildings of Equation (3) without any reference to the states of a power system. A novel occupancy-based HVAC control strategy is developed by embedding the occupancy prediction algorithm into a linear programming (LP) MPC framework. The objective of the proposed control strategy is to (a) address large scale simulation cost for multiple buildings by integrating LP, (b) counteract to the discomfort existing in the current baseline control by using rolling MPC window, and (c) minimize both electricity consumption and the expected occupant discomfort by introducing occupancy predictions.

The uniqueness of the large scale building-grid integration is that hundreds of buildings need to be simulated simultaneously. Classical MPC can be solved by many algorithms for an individual building, but these algorithms are not computationally cost efficient for large scale simulation. In this study, the authors explore a low computation way, the LP-MPC. The canonical form of the building cost function during the prediction horizon [0,t] in Equation (2) solved by LP is derived as follows:

$$\begin{aligned} &\text{minimize } C^T y \\ &\text{subject to } A_{eq} y = b_{eq}; \\ &lb \le y \le ub. \end{aligned} \tag{8}$$

Where:

- $y = [T^1_{wall}, T^1_{zone}, T^2_{wall}, T^2_{zone}, \dots, T^t_{wall}, T^t_{zone} P^1_{hvac}, \dots, P^{t-1}_{hvac}]$;
- $A_{eq} = \begin{bmatrix} \mathrm{I}_2 & 0 & \cdots & 0 & \cdots & 0 \\ -A^l_x & \mathrm{I}_2 & \cdots & -B^l_{u_x} & \cdots & \vdots \\ \vdots & \ddots & \ddots & \vdots & \ddots & \vdots \\ 0 & \dots & -A^l_x & \mathrm{I}_2 & 0 & -B^l_{u_x} \end{bmatrix}$;
- $b_{eq} = B^l_{w_x}[w^l_x(1), \dots, w^l_x(t-1)]$;
- $C = [0, \dots, 0, -1, \dots, -1]$ containing a length of $2t$ of zeros and a length of $t-1$ of negativee ones;
- $lb = [T^1_{min}, \dots, T^t_{min}, P^1_{min}, \dots, P^{t-1}_{min}]$;
- $ub = [T^1_{max}, \dots, T^t_{max}, P^1_{max}, \dots, P^{t-1}_{max}]$.

The linear optimization of Equation (8) will be solved by the simplex algorithm. To demonstrate the advantage of the proposed approach, a classic quadratic cost function using sequential quadratic programming is formulated to compare. The canonical form of the MPC based on Equation (2) is described as follows:

$$\begin{aligned} &\text{minimize } \textstyle\sum_0^{t-1}\{u_x + \gamma(x^l - T_d)^2\} \\ &\text{subject to } \dot{x}^l = A^l_x x^l + B^l_{u_x} u^l_x + B^l_{w_x} w^l_x; \\ &lb_x \le x^l \le ub_x; \\ &lb_u \le u^l_x \le ub_u. \end{aligned} \tag{9}$$

Where:

- $x^l = [T^1_{wall}, T^1_{zone}, T^2_{wall}, T^2_{zone}, \dots, T^{t-1}_{wall}, T^{t-1}_{zone}]$;
- $u^l_x = [P^1_{hvac}, P^2_{hvac}, \dots, P^{t-1}_{hvac}]$;
- The matrix form is the same from Equation (2) as A^l_x, $B^l_{u_x}$, and $B^l_{w_x}$;
- The bound settings such as lb_x, ub_x, lb_u and ub_u are same as the boundaries set in Equation (8).
- γ denotes a predefined penalty factor
- T_d denotes a desired room temperature set-point

An occupancy-based linear programming MPC is additionally developed to achieve the purpose of enabling more energy consumption savings. The authors introduce an occupancy-based slack relaxation of the constraints of Equation 8 to integrate the occupancy information. The occupancy information such as presence and absence is predicted based on a probabilistic occupancy modelling technique for commercial buildings (Reinhart, 2004). The model is redesigned in this study to focus on the occupancy status of building level. The model tends to simulate and predict the occupancy state in terms of group behaviors in an office environment. For example, the occupancy model will predict the lunch break as absence during certain time periods if the aggregated historical training data show a majority of the people leave the offices for lunch. Hence, the constraints on the states, namely $[{T_{max}}^1, \dots, {T_{max}}^t]$, will increase, which will sacrifice the individual comfort of people who still remain in the office at the lunch break time. Four occupancy-based control rules are proposed here: 1) if no people are present in one hour, the set-point upper bound will go up 5°F (2.77°C), 2) if people are going to leave within one hour, the set-point upper bound will go up 2°F (1.11°C), 3) if people are going to come in within one hour, the set-point upper bound will go down 2°F (1.11°C), and 4) if people are staying continuously for one hour, no change will be made on the bounds of the set point.

Second, the optimal control problem of the building-integrated power network is formulated. The issue of time-scales of the building-grid coupling is addressed by proposing the use of Gear's method. Note that when the building load is fed into Equation (4) of the grid, it is assumed that non-HVAC load will be scheduled and fixed and thus will be frequency insensitive as shown in Equation (5). Air conditioning as an optimization variable is isolated which is equivalent to the $U_X(t)$ in Equation (3). Then, a building-grid optimal MPC problem based on Equations (3) and (6) can be expressed as follows:

$$\text{minimize} \int_0^t \left(X_b^T Q_b X_b + c X_g^T Q_g X_g\right) dt$$

subject to

$$\begin{gathered} \dot{X_b}(t) = A_X X_b(t) + B_{u_X} U_X(t) + B_{w_X} W_X(t)\ ; \\ E\dot{X_g}(t) = A_g X_g + A_{hvac} U_{hvac}(t) + \\ B_m U_m(t)\ + B_F U_F(t) + B_{mi} W_{mi}(t); \\ lb_b \le X_b \le ub_b; \\ lb_g \le X_g \le ub_g; \\ lb_{ux} \le U_X = U_{hvac} \le ub_{ux}; \\ . \end{gathered} \tag{10}$$

Where:

- lb_b is the lower bound for the building states;
- ub_b is the upper bound for the building states;
- lb_g is the lower bound for the grid states;
- ub_g is the upper bound for the grid states;
- lb_{ux} is the lower bound for the building cooling power;
- ub_{ux} is the upper bound for the building cooling power;
- for remaining notations refer to Equations (3) and (6).

Building MPC Results

To demonstrate the effectiveness of the LP MPC, a sample building is used to compare the system performances of the 4 control strategies: a baseline bang-bang control, an LP MPC, a quadratic cost MPC, and an Occupancy-based LP MPC. The RC network model and the baseline bang-bang control of the sample building was previously validated by an earlier study (McFadden, 2015). All the controls are simulated from July 8th to July 13th of 2013. Weather information (outdoor air temperature and solar radiance) is retrieved from the National Oceanic and Atmospheric Administration (NOAA). The authors interpret the weather information for 5-min interval to match the control time steps. The internal heat gain is estimated from the power measurement and the operation schedules from the Building Management System of the sample building. The thermostat is set to be 72°F (22.22°C) with 2°F deadband (1.11°C) during daytime while the night setback allows it to go up to 75°F(23.88°C) with 4°F deadband (2.22°C). The occupancy schedules are predicted from the probabilistic model based on the historical occupancy information collected from multiple offices during the same period. Occupancy predictions are compared to the ground truth data collected from multiple sensors installed at different offices, shown in Figure 3. The numerical simulation results for buildings are presented in Figure 4 for the 200 kW peak building for July 9th.

The energy savings and comfort violations are presented in Table 1 and Table 2. The energy saving is calculated as follows:

$$\% = \frac{|MPC_i - Baseline_i|}{Baseline_i} \tag{11}$$

Where MPC is the MPC energy consumption and $Baseline$ is the bang-bang energy consumption at day i. To quantify the improvement of the proposed MPC control strategies over the traditional Bang-bang control, two discomfort indices are introduced as follows:

- Discomfort I (DI)

$$DI = \frac{\sum_{k=1}^{d} (T_{con}(k) - T_d(k))}{d} \tag{12}$$

- Discomfort II

$$DII = \frac{\sum_{k=1}^{d} |\Delta D|}{d} \tag{13}$$

$$\Delta D = \begin{cases} T_{con}(k) - T_{max} & T_{con}(k) > T_{max} \\ T_{min} - T_{con}(k) & T_{con}(k) < T_{min} \\ 0 & else \end{cases}$$

Where d is the evaluated time steps, T_{con} is the controlled room temperature, T_d is the desired set point temperature, T_{min} and T_{max} are the lower and upper constraints of the desired set point temperature.

Table 1 shows energy savings from July 8th to July 13th, evaluated by Equation (11). The simulation results do not indicate much saving from the quadratic MPC. LP MPC has some potential to save some energy consumption at certain days, such as July 8th. Occupancy-based LP MPC can achieve further saving, by a margin near 10%. The average saving is 80 kWh per day for simulated week compared to the baseline bang-bang control.

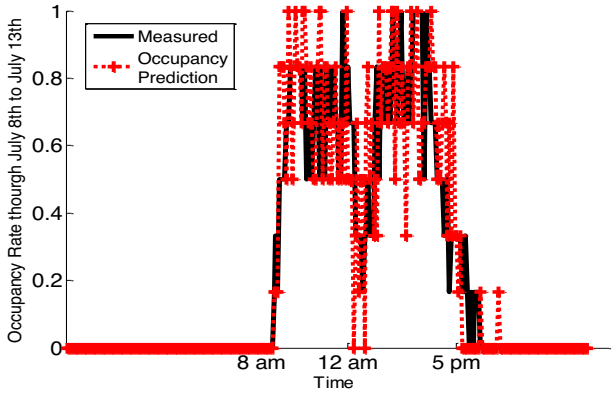

Figure 3: Occupancy Prediction.

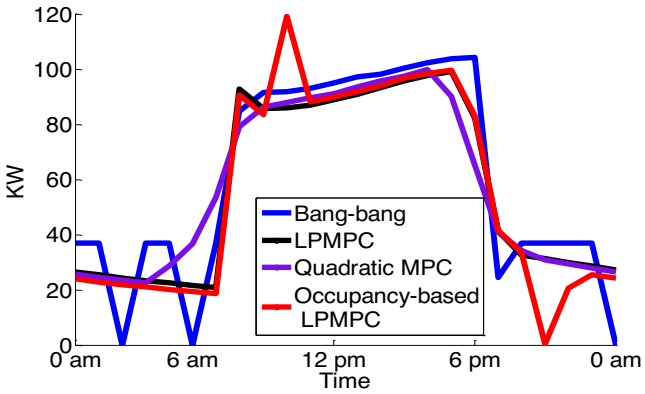

Figure 4: Energy performances for 4 strategies.

The authors additionally examine if the energy savings are achieved due to large violations of the occupants' comfort. The focus is only on the methods that demonstrate saving potentials, LP MPC and occupancy-based LP MPC. Two comfort indices, calculated daily from Equation (12) and Equation (13), are shown in Table 1 for the whole test week. The baseline is actually robust enough with a deviation range around 0.75℃ from the desired set point according to the comfort index DI. The violations above the upper and lower constraints are ranging around 0.09℃. The LP MPC has no violations at all for the upper and lower constraints of the set point, shown by DII. It allows more deviation from the set point (around 1.09℃) to save the energy consumption while maintains the room temperature in a comfort zone. Compared to the LP MPC, the occupancy-based LP MPC allow the system to respond to the unoccupied period which save even more energy consumption. However, the uncertainty of the occupancy prediction creates trouble to keep up the constraints. Nevertheless, the violations from the occupancy-based LP MPC is very similar to the baseline control. A more detailed view of the differences and advantages of the methods is shown at Figure 5. It shows the simulated room temperature at July 12th with 5-min control step. The baseline control and LP MPC do not respond to the occupancy and consume more energy before people arrive (9 am) and leave (5pm). Both methods also do not react to the lunch break, indicating low occupancy. In the contrast, the occupancy-based LP MPC violates some of the comfort constraints at afternoon (the third little peak of black line around 4 pm) and early morning (the arriving time after 9 am). It additionally misses a saving potential period around 1 pm (the second period of low occupancy rate after the 12 pm lunch break). These issues discovered during the occupancy-based control are owing to two reasons: 1) the Linear Programming is over relaxing the optimal solution of the zone temperature by the changes of the upper constraints, and 2) the uncertainty of the occupancy predictions misleads the control operations. Both problems can be solved by more accurate occupancy modelling and more reasonable set points for the unoccupied period.

The authors further introduce stochastic factors on both the building size, building thermal properties, and internal equipment schedules to simulate a cluster of 130 commercial buildings at July 9th. From analysis of the single building test results, the LP MPC and the Occupancy-based LP MPC is further used. The numerical simulation of total building load for 130 buildings at July 12th are presented in Figure 6.

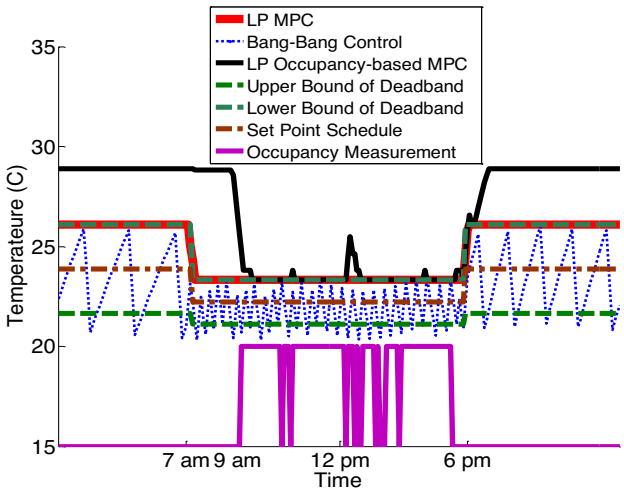

Figure 5: Zone temperature controls for Baseline, LP MPC, and Occupancy-based LP MPC at July 12th.

Table 1: Energy Savings per day comparing to bassline (the bang-bang control)

Methods	Quadratic MPC		LP MPC		Occupancy -based LP MPC	
	KWh	%	KWh	%	KWh	%
July 8th	22.79	1.71	74.53	5.59	124.6	9.95
July 9th	9.71	0.70	29.84	2.15	55.45	4.00
July 11th	4.37	0.32	12.98	0.95	19.98	1.46
July 12th	9.81	0.72	24.25	1.78	52.77	3.88
July 13th	20.22	1.46	35.19	2.54	63.42	4.57

Table 2: Comfort Violations per day.

Methods	Baseline		LP MPC		LP occupancy -based MPC	
	DI*	DII*	DI	DII	DI	DII
July 8th	0.76	0.10	1.10	0	1.18	0.08
July 9th	0.74	0.09	1.09	0	1.15	0.05
July 11th	0.76	0.10	1.10	0	1.50	0.40
July 12th	0.71	0.08	1.10	0	1.19	0.09
July 13th	0.78	0.08	1.05	0	1.19	0.14

*All units for DI and DII presented as °C.

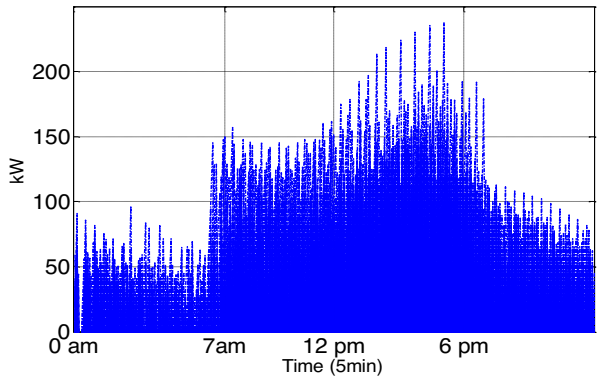

a) Baseline Bang-bang Control

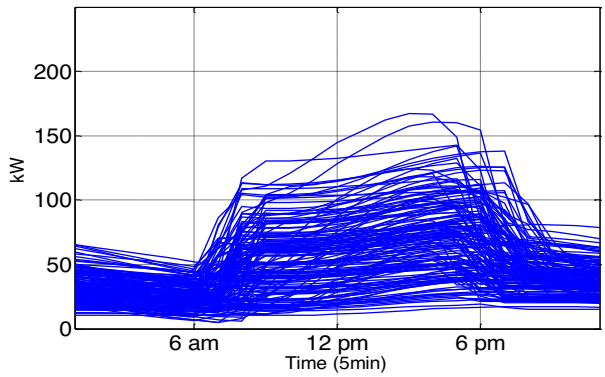

b) LP MPC

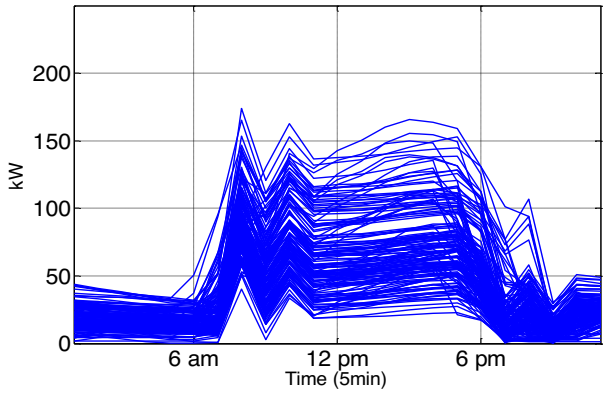

c) Occupancy-based LP MPC

Figure 6: Simulated Energy Profiles for the baseline control, the LP MPC, and Occupancy-based LP MPC.

Integration Grid Results

For building load, the occupancy-based LP MPC with 5 minutes rolling window is integrated. The MPC coupling of Equation (10) between the buildings and the grid regulate the grid frequency around the normal rate, 60 Hertz. Three communities (consisting respectively of 70,100, and 130 buildings) with maximum power peak around 400 kW for each individual building are simulated. These building loads are distributed to a power network of 9 grid buses. For each 5-minute building simulation step, Gear's method discretizes the swing equation to 10 secs for the operation of the buses. A quadratic program is used to optimize Equation (10) during the 5-min rolling window. The interior-point-convex option is selected for the *quadprog* optimization function in Matlab with violation threshold below 10^{-8} for the constraints. The first 35-minute integration between the building load and the grid's buses operations is shown in Figure 7.

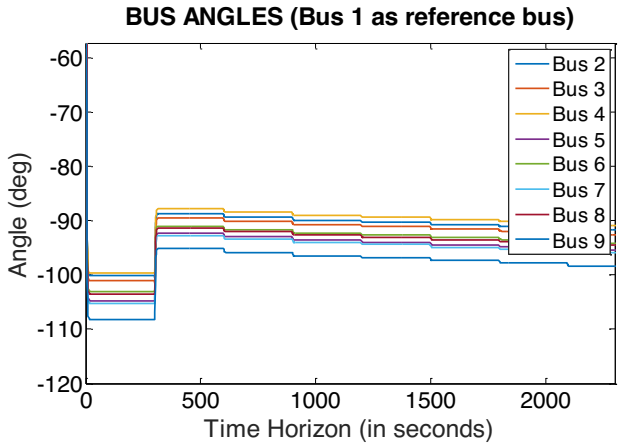

Figure 7: Stabilized buses' angle.

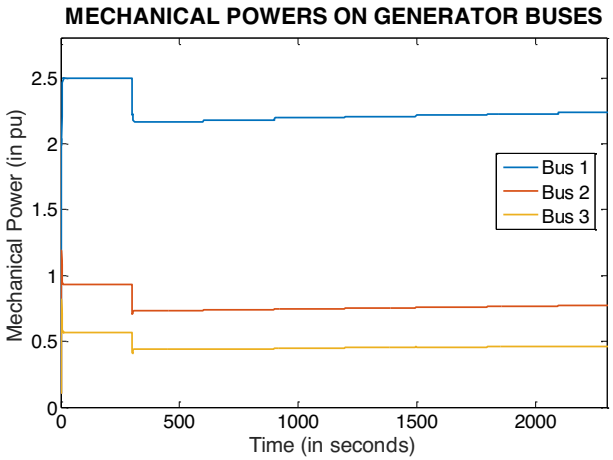

Figure 8: Distributed power from buses.

It is obvious from Figure 7 that the bus angles stabilized very quickly. Authors additionally check whether the buses reached the desired set points of power distributions by examining the trajectories for all the power supplied in terms of per-unit system (p.u.) in Figure 8. A per-unit system expresses a quantity as fraction of the defined based unit quantity. For this study, the base power is set to 100 MW. Figure 8 shows the first 3 buses' operation

trajectories. Although there are certain up and down ramps at the beginning seconds, all the buses stabilized quickly to reach the stabilized statuses.

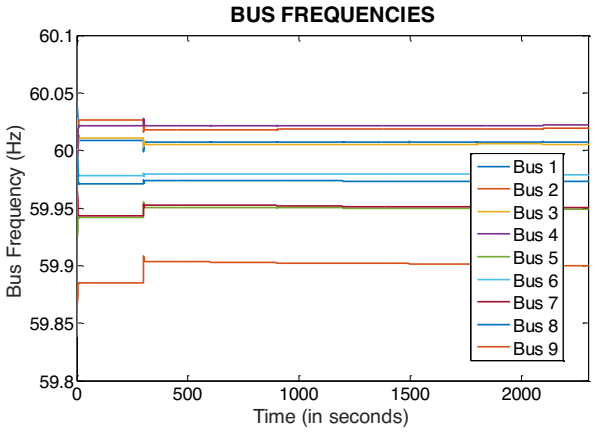

Figure 9: Simulation of 9 buses.

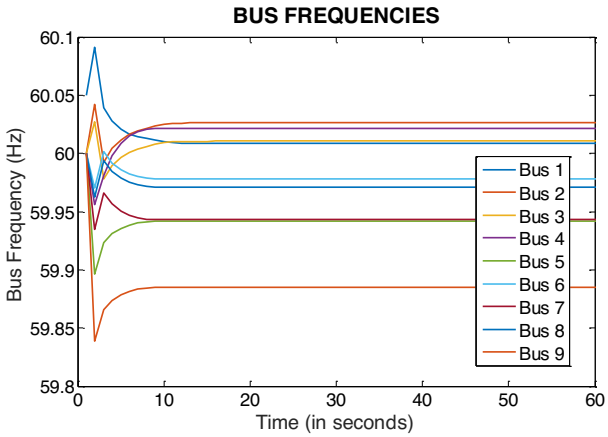

Figure 10: Beginning stage of the 9 buses.

All the frequencies of the 9 buses during the power balance operation are presented in Figure 9 and Figure 10. All buses are supposed to be maintained near 60 Hertz. Most of the buses are not deviated much from the 60 Hertz threshold. The reason for certain buses to have a bit of deviation of frequency threshold is owing to the loose constraints from the initial settings to find feasible solutions for Equation (10).

Discussions

The proposed building-grid integration with occupancy-based building control connects buildings, people, and grid in three levels. At the building level, several control strategies are demonstrated using state-of-the-art algorithms. Fast solvers should be always the first priority owing to the speciality of the computation scale to simulate hundreds of buildings. A new linear-programming based MPC approach is proposed. The improvement of control performances show different potentials of the energy consumption saving. At the people level, all the building control strategies are evaluated by two innovative discomfort indexes. Those discomfort indexes measure the violations between the maximum tolerance of the people comfort and the deviation from the desired comfort level. The building occupants' thermal comfort are maintained with the intelligent control of the HVAC system based on occupants' presence prediction. The uncertainty of the presence predictions cause most of the comfort level violations. However, no significant comfort violations could be observed for the proposed control strategy of the buildings. The last but not the least is the grid level. The building MPC generates load in community scale independently of grid with much slower time step. Coupling between the building load and the grid operation needs an alternative discretization approach to regulate the angles, the frequencies and the generating powers of the grid buses. By combining Gear's discretization with an MPC approach, the performances of the reliability and resiliency of the grid are quantified.

Conclusion

The proposed research in this paper expands traditional optimization and optimal control studies for buildings and power grids. The project develops: 1) an innovative modelling framework to control buildings in large scale based on linear programming, 2) integration of the occupancy modelling for building control, 3) and the design and coordination of coupled controls for a large-scale network of buildings and generator buses. The attempt to formulate such a complex sustainability problem as a coupled large-scale control problem creates a new paradigm for studies of the impacts of smart, connected communities on energy supply and demand along with operational stability of power networks.

Future studies need to be conducted to enhance the performance of this framework. First, the building models need to be developed based on more realistic examples by introducing 1) AHU models for commercial buildings and 2) compressor performance curve for residential buildings. Currently, authors are seeking for real test beds and data sources from SCE's Johanna and Santiago substations in Central Orange County of California. The smart test beds in the 2500 buildings of all the substations could also leverage the success of the decentralized and distributed approaches that are still under developing by authors. The final point is that the building-grid coupling controls tested now are linearized. It is very important to additionally address the nonlinearities of the buildings and the grid with novel modelling approaches. In conclusion, future studies will introduce more realistic nonlinear building and grid models in a larger simulation scale that truly represents a smart city scale, while advanced techniques are going to be developed to handle nonlinearities during the operation and uncertainty of the occupancy comfort violations. The work will be very useful in urban smart city planning, designing, and operation stages. Practical implementations are possible with real-time data fitting of the models and integration with high performance computing techniques.

Acknowledgement

This material is based upon work supported by National Science Foundation (NSF), under Grant No. CBET-1637249.

References

Lazaroiu, G. C., and M. Roscia. (2012). Defination methodology for the smart cities mode. *Energy* 47, 326-332.

Howard, B., Parshall, L., Thompson, J., and Hammer, S., Dickinson, J., and V., Modi. (2012). Spatial distribution of urban building energy consumption by end use. *Energy and Buildings 45*,141-151.

Heiple, S., and D.J. Sailor. (2008). Using building energy simulation and geospatial modeling techniques to determine high resolution building sector energy consumption profiles. *Energy and Buildings 40(8)*, 1426-1436.

Reinhart, C.F., and C.C. Davila. (2016). Urban building energy modeling a review of a nascent field. *Building and Environment 97*, 196-202.

Zhao, P., Henze, G., and M. Brandemuehl. (2015). Dynamic frequence regulation resources of commercial buildings through combined buildings system resources using a supervisory control methodology. *Energy and Buildings 86*, 137-150.

Blum, D., and L.M., Norford. (2014). Dynamic simulation of regulation demand response by HVAC systems. In *ASHRAE/IBPSA Building Simulation Conference*, Atlanta, GA, U.S.A.

Pisello, A., Bobker, M., and F., Cotana. (2012). A building energy efficiency optimization method by evaluating the effective thermal zones occupancy. *Energies 5*, 5257-5278.

Chatzivasileiadis, S., Bonvini, M., Matanza, J., Yin, R., Nouidui, T.S., Kara, E.C., Parmar, R., Lorenzetti, D., Wetter, M., and S. Killiccote. (2016). Cyber-Physical Modeling of Distributed Resources for Distribution System Operations. *Proceedings of the IEEE 104(4)*, 789-806.

ARPA-E. (2016). Arpa-e: Reimagining the u.s. electric grid. Available at : http://arpa-e.energy.gov/?q=news-item/arpa-e-reimagining-us-electric-grid.

Energyplus, Department of Energy. (2015). Available at: http://apps1.eere.energy.gov/buildings/energyplus/.

Equest, Department of Energy. (2016). Available at: http://doe2.com/equest/.

Dong, B., O'Neil, Z., Luo, D., and T., Bailey. (2014). Development and calibration of an online energy model for campus buildings. *Energy and Buildings 76*, 316-327.

Taylor, J. (2015). Convex Optimization of Power Systems. *Cambridge University press*.

Fosha, C., and Elgerd, O.I. (1970). The megawatt-frequency control problem: A new approach via optimal control theory. *Power Apparatus and Systems, IEEE Transactions on, 89(4)*, 563-577.

Elgerd, O.I., and C., Fosha. (1970). Optimum megawatt-frequency control of multiarea electric energy systems. *Power Apparatus and System, IEEE Transaction on, 89(4)*, 556-563.

Maasoumy, M., and A.S. Vincentelli. (2014). Comparison of control strategies for energy efficient building HVAC systems. In *Proceedings of the Symposium for Architecture & Urban Design*, San Diego, CA, U.S.A.

Ma., Y., Borrelli, F., Hencey, B., Packard, A., and S., Bortoff. (2009). Model predictive control of thermal energy storage in building cooling systems. In *Decision and Control, Proceedings of the 48th IEEE Conference on*.

Elmahdi, A., Taha, A.F., Sun, D., and J.H. Panchal. (2015). Decentralized control framework and stability analysis for networked control systems. *Journal of Dynamic Systems, Measurement, and Control 137(5)*, 051006.

Taha, A.F., Elmahdi, A., Panchal, J.H., and D. Sun. (2015). Unknown input observer design and analysis for networked control systems. *International Journal of Control 88(5)*, 920-934.

Gatsis, N., and G.B. Giannakis. (2012). Residential load control: Distributed scheduling and convergence with lost AMI messages. *IEEE Transaction on Smart Grid 3(2)*, 770-786.

Gatsis, N., and A.G. Marques. (2014). A stochastic approximation approach for load shedding in power networks. In *Proc. IEEE International Conference on Acoustics, Speech, and Signal Processing,* Florence, Italy.

Gatsis, N., and G.B. Giannakis. (2013). Decomposition algorithms for market clearing with large-scale demand response. *IEEE Transaction on Smart Grid 4(4), 1976-1987.*

Zhang, Y., Gatsis, N., and G. Giannakis. (2013). Disaggregated bundle methods for distributed market clearing in power networks. In *Proc. IEEE Global Conference on Signal and Information Processing (GlobalSIP)*, Austin, TX, U.S.A.

Bazrafshan, M., and N. Gatsis. (2016). Decentralized stochastic optimal power flow in radial networks with distributed networks. *IEEE Transactions on Smart Grid 99*, 1-15

Reinhar, C.F. (2004). Lightswitch-2002: a model for manual and automated control of electric lighting and blinds. *Solar Energy 77(1)*, 15-28.

Mcfadden, G., Li, Z.X., Dong, B., and R. Vega. (2015). HVAC Load Forecasting using LIDAR data and

physics-based models. In *ASHRAE Winter Conference*, Chicago, IL, U.S.A.

.